Lowland Technology International 2017; 20 (1): 1-14
International Association of Lowland Technology (IALT): ISSN 1344-9656

Research Paper

Reconfirmation of Skempton-Bjerrum 2D to 3D settlement conversion using FEM of full scale embankments

S. Chaiyaput [1] and D.T. Bergado [2]

ARTICLE INFORMATION

Article history:

Received: 27 July, 2017
Received in revised form: 10 December, 2017
Accepted: 15 December, 2017
Publish on: 01 June, 2018

Keywords:

2D FEM
3D FEM
Skempton-Bjerrum
Settlement
Embankment

ABSTRACT

The soil is a production of natural process, which is highly variable with very complex properties, and soil behavior can be difficult to calculate. Numerical Simulation can be applied to deal with the numerous aspects of complex geotechnical structures. The 3D FEM simulation model can present the conditions of the geotechnical project in details and assumptions, which are similar to actual situations, but the process of running the 3D FEM analysis takes longer computer time. Therefore, 2D FEM simulation model is proposed to reduce calculation time, but the prediction results are usually overestimated. Accordingly, this paper re-analyzed the 2D analysis to represent the performance of 3D analysis based on Skempton-Bjerrum method. The simulated 2D and 3D FEM settlement results had been carried out and compared with the measured data of two full scale embankments including the dissipation of the excess pore pressure. Consequently, it was confirmed that predicted result of 2D and 3D FEM numerical simulation agreed with the correction of Skempton-Bjerrum method that can be applied to predict the final settlements in 3D conditions.

1. Introduction

The range of soil properties can be large variation and tremendous. Moreover, the properties can change with many factors such as time, stress or even moisture, this means that the opportunity of working with widely scattered data cannot be avoided. While, the construction design requires accurate results for a good calculating of engineering design and a clear understanding of complicated problems. Therefore, there are several methods, which are described from basic formulas to advanced finite element analysis, have been investigated for considering a construction process.

The concept of consolidation settlement was introduced by Skempton-Bjerrum (1957). They proposed a correction factor (μ) to analysis the settlement from the dissipation of excess pore pressure.

The finite element method (FEM) has become popularly applied for studying behavior of geotechnical structure as a continuum model (Bergado et al., 1995; Bergado et al., 2000; Lai et al., 2006; Tanchaisawat et al., 2009). Especially, the three-dimensional finite element model (3D FEM model) that can simulate the construction project in details and assumptions, which are similar to actual situations such as construction method, material properties, acting loads, and geology. These factors are important for the calculation process in order to increase model efficiency. Nevertheless, the 3D FEM, which is difficult in creating a model, is sometimes confused with a complex condition. Processing time may take from

[1] Lecturer, Department of Civil Engineering, Faculty of Engineering, King Mongkut's Institute of Technology Ladkrabang, 1 Soi Chalongkrung 1, Chalongkrung Rd., Ladkrabang, Bangkok 10520, THAILAND, salisa.fern@gmail.com, salisa.ch@kmitl.ac.th
[2] Professor Emeritus, Geotechnical and Earth Resources Engineering, School of Engineering and Technology, Asian Institute of Technology, Klongluang, Pathumthani 12120, THAILAND, dbergado@gmail.com
Note: Discussion on this paper is open until December 2018.

several minutes to a day. Consequently, many researchers conduct the simulation by modelling only 2D FEM model based on the condition of continuous structure to reduce the time of analysis.

Bergado and Teerawattanasuk, (2008), and Teerawattanasuk, (2004) investigated the geometric effects of the reinforced embankment corresponding to 2D and 3D conditions. The 2D FEM analysis (**Fig. 1**) can present the behavior of long embankment (length-to-width ratio of 3.0), while the FEM 3D analysis (**Fig. 2**) can capture the behavior of short embankment (length-to-width ratio of 1.0).

For the construction design, the settlement is an important factor to consider as a design criterion, especially on soft ground conditions. Subsequently, the behavior of reinforced earth structure on soft ground, and its influence factors have been analyzed using finite element method (FEM) by several researchers (Rowe and Ho, 1997, Long, 1996; Chai, 1992; Hird and Kwok; 1989, etc.). Jostad (2016) developed the calculation tool for consolidation settlement analysis based on 3D finite element model.

The aim of this research is reconfirming the prediction the 2D to 3D conversion of final settlements by using the method by Skempton and Bjerrum (1957) with the final settlements calculated by 2D and 3D FEM simulations of the 2 full scale embankments on soft Bangkok clay.

2. Total settlements

Total ultimate settlement is the total compression of a structure on soft ground foundation. The ground settlement is an important factor to consider as a design criterion on embankment construction on soft ground. The total settlements can consist of three separate components of settlement as follows:

$$\rho_t = \rho_i + \rho_c + \rho_s \quad [1]$$

where: ρ_t = total ultimate settlement,

ρ_i = immediate settlement resulting from the constant volume compression of soft ground at undrained condition,

ρ_c = consolidation settlement resulting from the time dependent flow of water from the loaded soft ground due to the dissipation of excess pore pressure,

ρ_s = secondary settlement or creep which is also time dependent but may occur at essentially constant effective stress.

2.1 Consolidation settlements

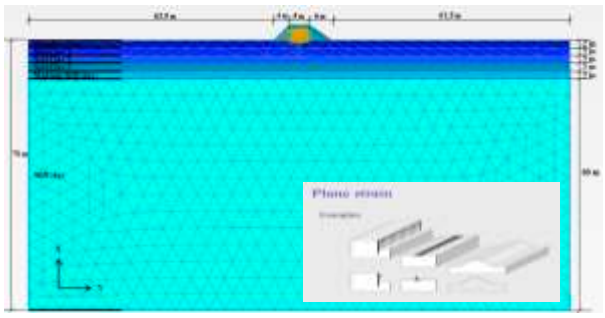

Fig. 1. The simulation model in PLAXIS 2D.

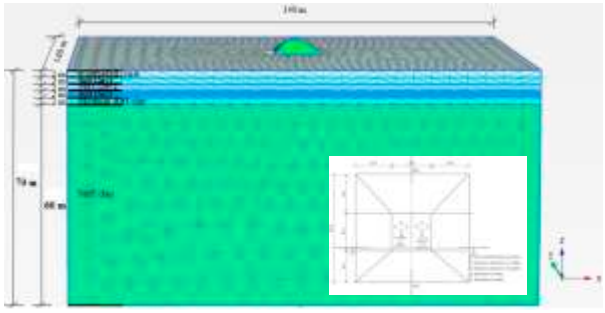

Fig. 2. The simulation model in PLAXIS 3D.

The field observation on various instrumented test has founded that almost all clays demonstrate a maximum past pressure, σ_p, the magnitude of which depends on the plasticity and geological history of the clay deposit (Bjerrum, 1972).

For increment of loading within the range of maximum past pressure, σ_p, its settlement is small, the excess pore pressure is small and it dissipates rapidly. For loads that exceed maximum past pressure, σ_p, the settlement is high, the excess pore pressure is high and dissipate slowly. Hence, the embankment settlement can be analyzed in two scenarios. If the stress in the clay is lower than σ_p, the consolidation settlement can be predicted from the equation, defined as:

$$\rho_c = \mu \sum_o^z m_v \Delta\sigma d_z \quad [2]$$

In cases, however, in which the stresses in the clay exceed σ_p, the consolidation settlement is composed of two contributions. The first contribution settlement occurring when the load is increased from σ_{vo} to σ_p, calculated as:

$$\rho_{c1} = \mu \sum_o^z m_v (\sigma_p - \sigma_{vo}) d_z \quad [3]$$

The second contribution is the consolidation settlement which occurs when σ_p is exceeded is shown as:

$$\rho_{c2} = \mu \sum_{o}^{z} \frac{C_c}{1+e_o} \log \frac{\sigma_p + \Delta\sigma d_z}{\sigma_p} \quad [4]$$

The total consolidation settlement, therefore, is the sum of the two settlement contributions:

$$\rho_c = \rho_{c1} + \rho_{c2} \quad [5]$$

3. Method of Skempton and Bjerrum (1957)

Skempton and Bjerrum (1957) made a contribution to settlement analysis by pointing out that an element of soil underneath a foundation undergoes lateral deformation as a result of applied loading and that the induced pore water pressure is in general less than the increment in vertical stress on the element, because it is dependent on a function of the pore pressure coefficient, *A* (Skempton, 1954). The excess pore pressure set up may represented by the expression:

$$\Delta u = B \cdot \left[\Delta\sigma_3 + A \cdot (\Delta\sigma_1 - \Delta\sigma_3)\right] \quad [6]$$

where: $\Delta\sigma_1, \Delta\sigma_3$ = the increase in the principle stresses caused by loading

A, B = the pore pressure coefficients

For saturated clay, *B* = 1 and the value of *A* can be determined from pore pressure measurements in undrained triaxial tests. In one-dimensional consolidation tests, there is no lateral yield of soil specimen and the ratio of the minor to major principal effective stresses, K_o, remains constant. In that case, the increase of pore water pressure due to an increase of vertical stress is equal in magnitude to the latter. However, in reality the final increase of major and minor principal stresses due to a given loading condition at a given point in a clay layer do not maintain a ratio equal to K_o. This causes a lateral yield of soil. The increase of pore water pressure at a point due to a given load is:

$$\Delta u = \Delta\sigma_3 + A \cdot (\Delta\sigma_1 - \Delta\sigma_3) \quad [7]$$

Skempton and Bjerrum (1957) proposed that the vertical compression of a soil element of thickness d_z due to an increase of pore water pressure Δu may be given by:

$$d\rho_c = m_v \Delta u dz \quad [8]$$

where: m_v, is the coefficient of volume compressibility, or

$$d\rho_c = m_v \left[\Delta\sigma_3 + A(\Delta\sigma_1 - \Delta\sigma_3\right] dz \quad [9]$$

$$= m_v \Delta\sigma_1 \left[A + \frac{\Delta\sigma_3}{\Delta\sigma_1}(1-A) \right] dz \quad [10]$$

The preceeding equation can be integrated to obtain the total consolidation settlement:

$$\rho_c = \int_0^{H_t} m_v \Delta\sigma_1 \left[A + \frac{\Delta\sigma_3}{\Delta\sigma_1}(1-A) \right] dz \quad [11]$$

For conventional one-dimensional consolidation (K_o condition), which is equivalent to the 2D plane strain condition, the settlement or vertical compression is given as:

$$\rho_{c(oed)} = \int_0^{H_t} m_v \Delta\sigma_1 dz \quad [12]$$

Since the consolidation of a clay results from the dissipation of excess pore pressure, Skempton and Bjerruin (1957) proposed that a correction factor (μ) should be applied to the settlement calculated on the basis of oedometer test and showed that μ factor is a function of the geometry of the problem and the *A* value (**Fig. 3**). The *A* value decrease with OCR as tabulated in **Table 1.**

The correction factor μ decreases with OCR as indicated in **Fig. 4.** The equivalent 3D field settlement, ρ_c, is then equal to μ times the settlement calculated on the basis of oedometer tests $\rho_{c(oed)}$, which is equivalent to 2D plane strain condition for long embankment configuration (**Fig. 1**) as follows:

$$\rho_c = \mu \cdot \rho_{c(oed)} \quad [13]$$

The final primary consolidation, ρ_c, is calculated from

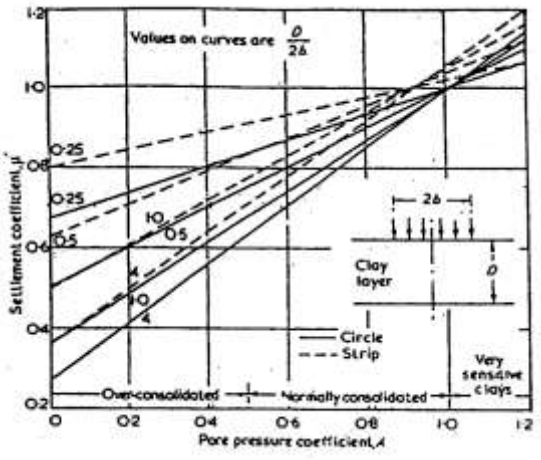

Fig. 3. Correlation factor for pore pressures set up under a foundation (Skempton and Bjerrum, 1957).

three-dimensional excess pore pressure obtained under undrained axisymmetric triaxial stress conditions, which is equivalent to 3D embankment configuration (**Fig. 2**).

3.1 Excess pore water pressures

The increase of pore water pressure in the soil due to various loading conditions without drainage is important in both theoretical and applied soil mechanics. If the load is applied very slowly on a soil such that sufficient time is allowed for pore pressure to drain out, there will be practically no increase of pore pressure. However, when a soil is subjected to rapid loading and if the permeability is small, there will be insufficient time for drainage of pore pressure. This will lead to an increase of the excess pore pressure. The excess pore pressure, u , generated beneath the embankment can be calculated by:

$$u = \mu\sigma_v \qquad [14]$$

where: μ = the pore pressure correlation factor

σ_v = the increase in vertical stress due to embankment loading effective vertical stress

Skempton and Bjerrum (1957) suggested that μ is a function of geometry of loading pore pressure coefficient A (**Fig. 3**) and OCR (**Fig. 4**).

4. Finite element modeling of reinforced embankment

The finite element method (FEM) has been used in many fields of engineering practice. Moreover, the FEM are using widely for analyzing geotechnical engineering projects, especially adopted to analyze the deformation and stability in geotechnical problems. Due to geotechnical applications require advanced constitutive models for the simulation of the non-linear and time-dependent behavior of soils. Moreover, the feature of the FEM software is equipped with special features to deal with the numerous aspects of complex geotechnical structures, multiphase analysis materials, special analysis procedures (e.g. hydrostatic, non-hydrostatic pore pressures, soil structure interaction, etc.). Therefore, the numerical modeling of the reinforced test embankment on soft foundation was performed using a finite element software.

4.1 Finite element simulation

The numerical modeling of the full-scale test embankment was performed using a finite element software. Two-dimensional simulation was modeled as a plane strain axisymmetric idealization, two-dimensional problem for finite element analysis consisting of x and y directions of long embankment, including simulation of construction sequence as shown in **Fig. 1.** The 3D finite element analyses had been carried out to investigate the behavior of embankment when it is subjected to loading of short embankment. Determination of accurate effective stresses is an essential task to accomplish this objective. Complex geotechnical structure can be solved with special features built within the program. The 3D finite element model is created through a two-dimensional (2D) in vertical cross-section model in x-y plane and later extended into the third dimension (z-direction) as shown in **Fig. 2.** Therefore, the geometric effects and plan dimensions of the test embankment, should be considered as important factors that can affect the results of the numerical simulations, which are compared with the prediction results using Skempton and Bjerrum correction.

Table 1. Caption Typical values of the pore pressure coefficient 'A' for working range of stress below foundation (Skempton and Bjerrum, 1957).

Type of Clay	A
Very Sensitive Soft Clays	> 1
Normally Consolidated Clays	0.5 – 1
Overconsolidated Clays	0.25 – 0.5
Heavily Overconsolidated Sandy Clays	0.00 – 0.25

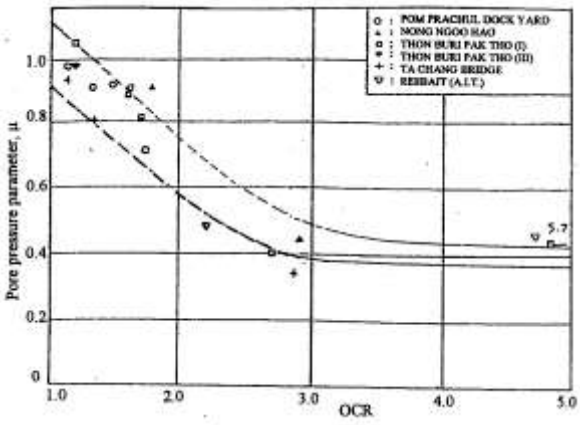

Fig. 4. Relationship between pore pressure parameter, μ, and over consolidation ratio for soft Bangkok clay (Balasubramaniam, 1985).

4.2 Finite element analysis of consolidation

Due to the feature of the FEM program, consolidation is used to perform time dependent settlement analysis under loading. Consolidation analysis corresponds to a coupling between the laws governing the behavior of the skeleton of the soil and the flow of pore fluid. In a

variation form, the analysis of this problem leads to the search for a field of displacements and a distribution of hydraulic head satisfying the simultaneous equation. Biot's consolidation theory (Biot, 1941) is a rigorous solution to this problem, when the soil skeleton is linear elastic and the pore fluid is incompressible. The equation used in the application for finite element analysis is shown below (Vermeer and Brinkgreve, 1995):

$$\nabla^T \left(\frac{k_p}{\gamma_w} \right) \nabla \left(\gamma_w - p_{steady} - p \right) - m^T \frac{\partial \varepsilon}{\partial t} + \frac{n}{k_w} \frac{\partial p}{\partial t} = 0 \qquad [15]$$

where: k_p is the permeability matrix

$$k_p = \begin{pmatrix} k_x & 0 \\ 0 & k_y \end{pmatrix} \qquad [16]$$

where: k_x = permeability in x-direction
k_y = permeability in y-direction
$p, p_{steady\ state}$ = pore water pressure
n = porosity
ε = strain tensor
k_w = *bulk modulus of water*

In general, when a nonlinear material model is used, iteration is needed to arrive at the correct solution. In finite element analysis, the consolidation for finite element analysis can be obtained using standard isoparameter finite element formulation procedure (Britto and Gunn, 1987).

5. Full scale test embankments

Two full scale proposed method test embankments

Fig. 5. Completed LLGs reinforced embankment construction.

on soft ground at AIT campus were utilized to evaluate and confirmed the final settlement predictions of 2D and 3D conditions.

5.1 LLGs reinforced embankment

The site of LLGs reinforced full scale test embankment (**Fig. 5**) was located in the campus of the Asian Institute of Technology (AIT), Klongluaung, Pathumthani, Thailand (Chaiyaput et al, 2014). The general soil profile and soil properties of the subsoil in the uppermost three layers at the AIT campus are presented in **Fig. 6.** The uppermost 10 m can be divided into 3 layers. The uppermost layer is weathered crust forms that consist of heavily overconsolidated reddish brown clay forms the uppermost 2 m. The second layer down to an approximate 8 m depth, this layer is soft clay layer. The medium stiff clay layer with silt seams and fine sand lenses was found at 8 to 10 m depth. Nether medium stiff clay layer is stiff clay layer.

The height of embankment was 4.0 m and was

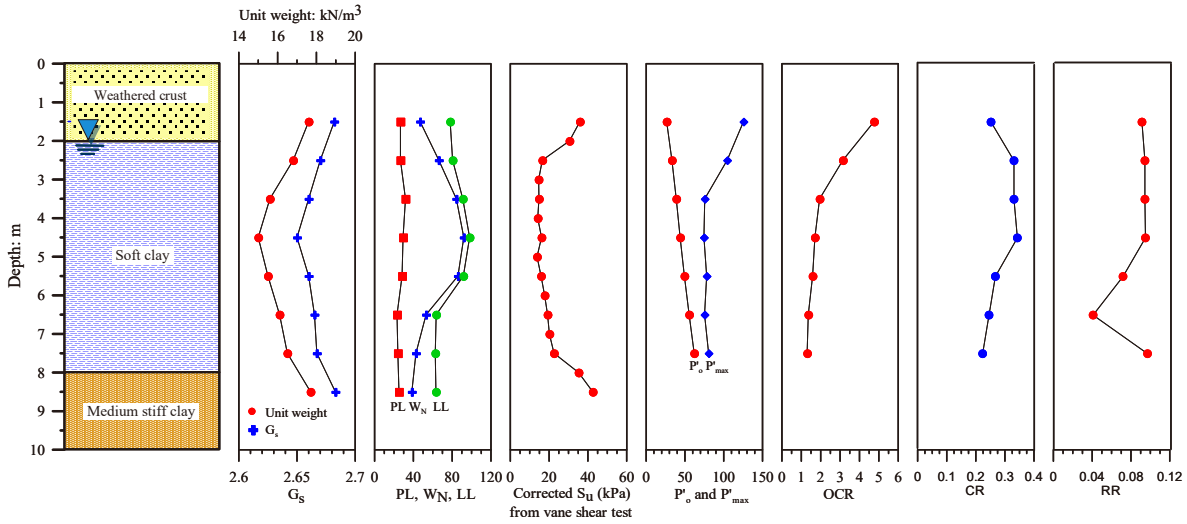

Fig. 6. The Soil profile and soil properties at the site.

constructed using silty sand backfill until 3 m height with six layers of plain pattern of Kenaf LLGs reinforcements. The vertical spacing of reinforcement was 0.5 m, and 1.0 m thick weather crust of soft Bangkok clay covered the silty sand backfill embankment to a total height of 4.0 m. Moreover, the side slope consisted of 1.0 vertical to 1.5 horizontal and back slope consisted of 1.0 vertical to 1.0 horizontal. The Kenaf LLGs opening size 4 mm was applied as reinforcement material, consisting of coated and non-coated (with polyurethane). The Kenaf LLGs dimensions were 1.0 m wide by 5.0 m long. The instrumentations in the subsoil were installed prior to the construction of reinforced embankment consisting of the surface settlement plates, subsurface settlement plates at 3 and 6 m. depth, and piezometers at 3 and 6 m. depth. The embankment plan view, section A-A and section B-B are shown in **Figs. 7, 8,** and **9,** respectively. The embankment was instrumented with settlement plates and piezometers to measure the surface settlements, subsurface settlements and excess pore water pressures of the reinforced embankment.

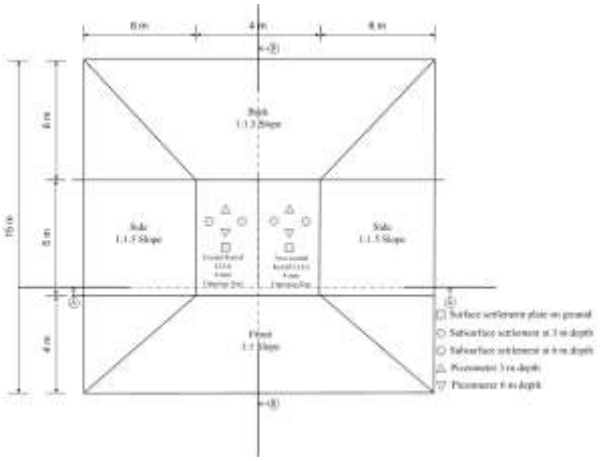

Fig. 7. Plan view of test embankment.

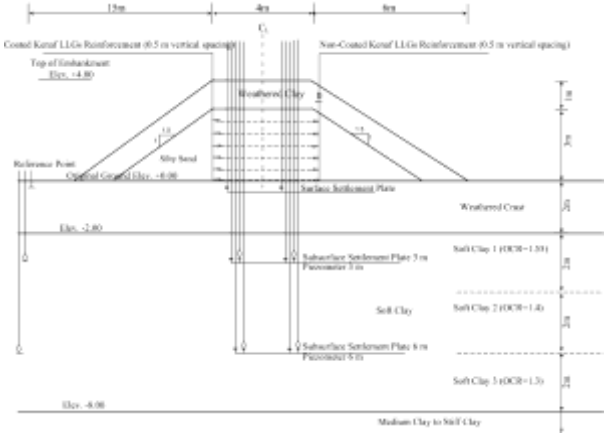

Fig. 8. Section A-A view of test embankment.

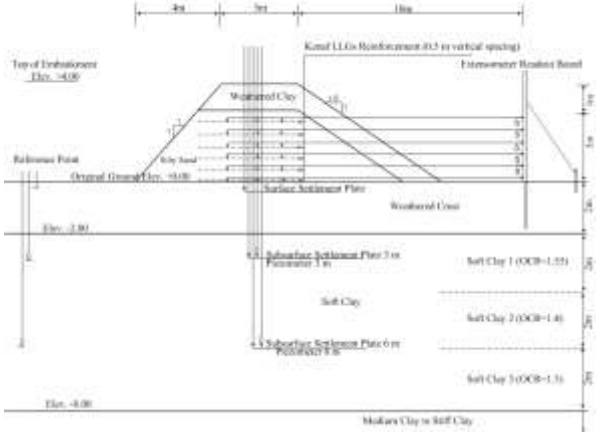

Fig. 9. Section B-B view of test embankment.

5.1.1 Finite element simulation

The numerical simulations of the full scale test embankment was performed by finite element method (FEM) using 2D and 3D softwares. The embankment was simulated as a plane strain, 2D problem as shown in **Fig. 1** as well as 3D problem as shown in **Fig. 2.**

The material properties of the backfill for the FEM simulations are tabulated in **Table 2.** The compacted sand and the compacted weathered crust of soft Bangkok clay were used for backfill soil in the embankment. The Mohr–Coulomb model with drained behavior was used for this backfill material. The friction angle and cohesion of silty sand and weathered crust were obtained from large scale direct shear test, cohesion, *c*'= 11.3 kPa and friction angle, φ' = 35.63 degrees for compacted sand and cohesion, *c*'= 10.0 kPa and friction angle, φ' = 26.00 degrees for weathered crust. Moreover, interface coefficient of silty sand 0.8 was used for analyses. The additional material parameters for FEM analyses were elasticity, E' = 7500 kPa, 3000 kPa, and Poisson's ratio, ν' = 0.30, 0.25 for the compacted sand and the compacted weathered crust, respectively.

Under the staged construction feature of the software, the incremental fill placement was simulated. During this construction stage, undrained analysis was applied to simulate the layer by layer construction. After the completion of the full height of the embankment, drained analysis was applied to simulate the consolidation process. Comparisons were done between observed field data and predicted results on surface settlement, subsurface settlement, and excess pore water pressures.

5.1.2 Settlement

The observed surface and subsurface settlements of the full scale test embankment using Kenaf LLGs reinforcement at coated and non-coated Kenaf LLGs sides were recorded and analyzed. During the

Table 2. Soil models and parameters used in FEM simulation on full scale LLGs test embankment.

Materials	Depth (m)	Model	Material behavior	γ_{sat} (kN/m^3)	γ_{unsat} (kN/m^3)	$k_x = k_z$ (m/day)	k_y (m/day)	E'ref (kPa)	v'	λ*	κ*	c' (kPa)	φ' (deg)	OCR
Subsoil														
Weathered crust	0 - 2	MCM	undrained	17	15	0.002	0.001	3000	0.25			10	23	
Soft clay 1	2 - 4	SSM	undrained	15	13	0.0008	0.0004			0.14	0.028	3	23	1.55
Soft clay 2	4 - 6	SSM	undrained	15	13	0.0008	0.0004			0.14	0.028	3	23	1.4
Soft clay 3	6 - 8	SSM	undrained	15	13	0.0008	0.0004			0.14	0.028	3	23	1.3
Medium stiff	8 -10	MCM	undrained	17	15	0.0004	0.0002	5000	0.25			10	25	
Stiff clay	10-30	MCM	undrained	19	17	0.004	0.002	9000	0.25			30	26	
Embankment														
Sand		MCM	drained	20	18	1	1	7500	0.3			11.3	35.63	
Clay		MCM	drained	16	15	0.002	0.001	3000	0.25			10	26	

R_{in}: Interface Coefficient; SSM: soft soil model; MCM: Mohr-Coulomb model.

construction, the rates of settlement slowly increased, and immediate elastic settlements occurred. After construction, the rates of settlement rapidly increased to 250 days from the end of construction. At 250 days after construction period, the settlements on coated Kenaf LLGs side at the surface, 3m and 6m depths were 295mm, 179mm and 79mm, respectively. The corresponding of settlements in non-coated Kenaf LLGs side at the surface, 3m and 6m depths were 298mm, 183mm and 82mm, respectively. Similar magnitudes of settlement rates were obtained in coated and non-coated Kenaf LLGs reinforcements.

Beneath the center point of coated and non-coated Kenaf LLGs reinforced embankment, the predicted results by FEM 2D and FEM 3D analyses were compared with observed field settlement data at surface (0.2m depth below the ground surface) and at subsurface (3m and 6m depth below ground surface) as illustrated in **Figs. 10, 11,** and **12,** respectively. The rates of settlement from FEM 2D method were higher than observed settlement data while the FEM 3D predictions generally agreed with observed settlements at the surface, 3m and 6m depth due to the fact that the three-dimensional loading condition is closer to the field condition. The predicted values of surface and subsurface settlements from FEM simulations were influenced by the boundary value problem (Auvinet and Gonzalez, 2000). Furthermore, the observed settlements apparently were more related to 3D than 2D conditions because of its symmetry and plan dimensions of the test embankment (Bergado and Teerawattanasuk 2008). Therefore, the effect of boundary conditions (2D and 3D) applied in numerical analysis can be considered to be an important factor that influence the predicted results due to the plan view dimensions as indicated in **Figs. 1,** and **2.** the 2D FEM simulations overpredicted the total settlements from the 3D FEM simulations by 28%, 27%, and 25%, respectively, corresponding to the surface, 3m and 6m depths.

According to Skempton and Bjerrum (1957) method, a correction factor (μ) can be applied to the settlement calculated on the basis. The correction factor (μ) decreases with increasing overconsolidation ratio (OCR). The correction factor (μ) at the surface 3m depth and 6m depth were 0.72, 0.73 and 0.75, respectively, which are equivalent to differences of 28%, 27% and 25% between 3D and 3D predicted settlement as shown in **Figs. 13.** Similarly, the difference between FEM 2D and FEM 3D simulation at the surface, 3m and 6m depths were 28%, 27% and 25%, respectively, as indicated in **Figs. 10, 11,** and **12.**

5.1.3 Excess pore water pressure

The full scale test embankment constructed on soft Bangkok clay foundation generated the build up of excess pore pressures. During the consolidation settlements, the excess pore pressure in the soft clay started to dissipate with time. Four open standpipe piezometers were used to monitor excess pore water pressure beneath the reinforced embankment at 3 m and 6 m depths. After 7 days from the end of construction (at full height of embankment), the excess pore water pressures rapidly increased to the maximum value of pore water pressure. The excess pore water pressures dissipated very fast with time after 15 days to 120 days and dissipated with slower rate after 120 days. After 240 days, the maximum excess pore water pressures decreased to 10 kPa and it was almost constant with time. The maximum excess pore water pressures on coated and non-coated kenaf LLGs side at 3m depth were 37 kPa and 35 kPa, respectively, at 7 days from the end of construction (**Fig. 14**). The maximum excess pore water

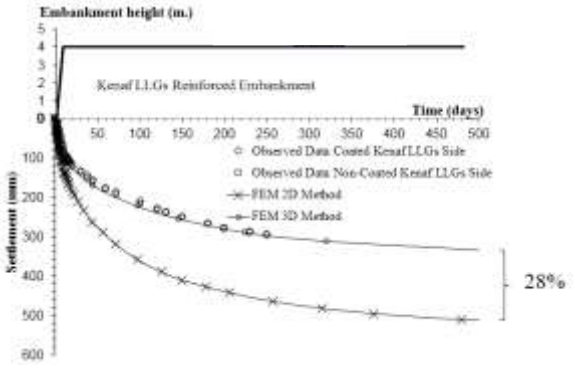

Fig. 10. Surface settlement (0.2m depth below the ground surface).

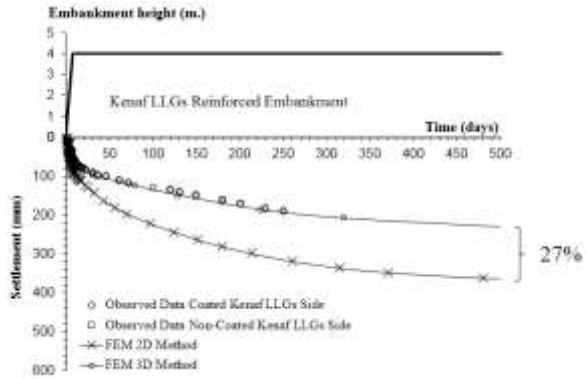

Fig. 11. The Subsurface settlement (3m depth below the ground surface).

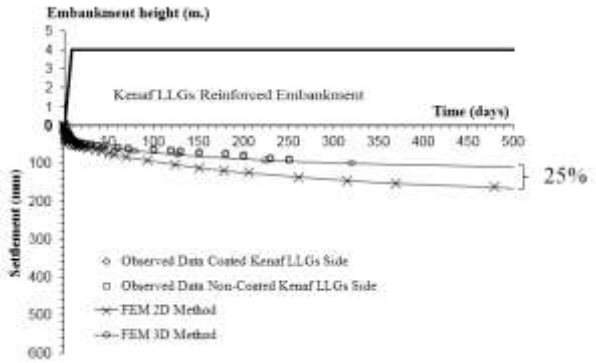

Fig. 12. The Subsurface settlement (6m depth below the ground surface).

pressures in coated and non-coated Kenaf LLGs side at 6m depths were 33 kPa and 32 kPa, respectively, at 7 days from the end of construction (**Fig. 15)**. The results between coated and non-coated LLGs sections were similar in magnitudes of excess pore water pressures in both 3m and 6m depths.

In case of simulated data, the maximum pore water pressures at 3m depth were 49 kPa and 34 kPa for FEM 2D and FEM 3D, respectively. From numerical simulation results at 6m depth, the maximum pore water pressures were 46 kPa and 32 kPa, for FEM 2D and FEM 3D, respectively. It can be seen that the predicted maximum excess pore-water pressure at the locations of 3m and 6m depths obtained from FEM 2D analyses

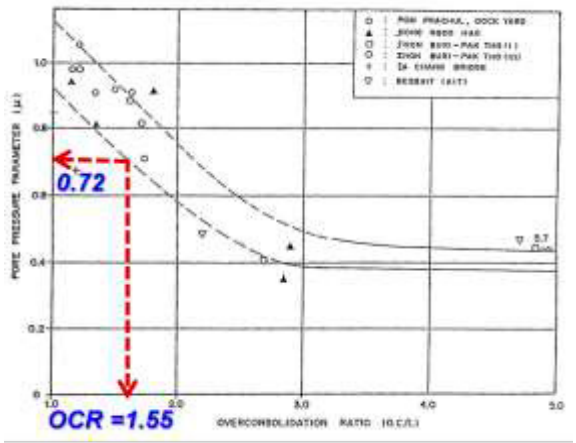

(a) at surface

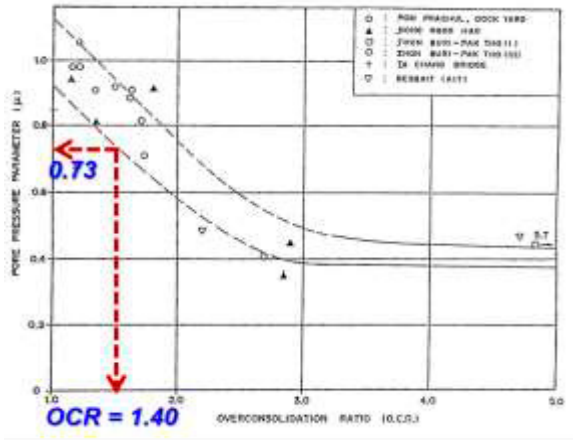

(b) at 3m depth

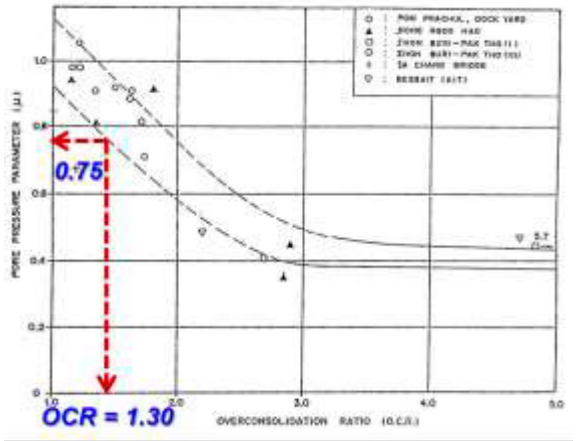

(c) at 6m depth

Fig. 13. The correction factor (μ) with overconsolidation ratio of Kenaf LLGs reinforced embankment.

overestimated the measured field data. The maximum pore water pressures from observed field data were slightly higher than FEM 3D and tend to agree and closely follow the FEM 3D predictions.

The excess pore water pressure form FEM 3D simulation yielded satisfactory agreement with the observed data because the test embankment has 3D configuration. The rate of dissipation for 2D simulation is lower than FEM 3D simulations. In the FEM 2D

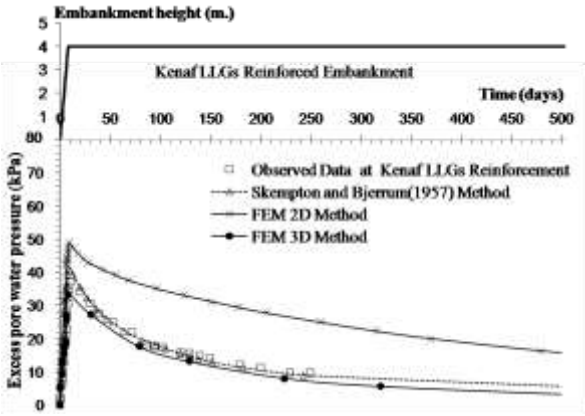

Fig. 14. Observed and predicted average excess pore pressure at 3m depth.

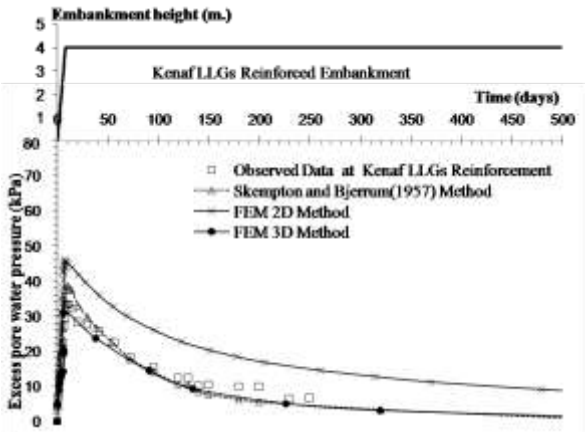

Fig. 15. Observed and predicted average excess pore pressure at 6m depth.

simulation, the excess pore water pressure can dissipate only in two-directions (x and y directions). However, the excess pore water pressure of FEM 3D condition can conveniently dissipate in three-directions (x, y, and z directions).

According to Skempton and Bjerrum(1957) method, a correction factor (μ) can be determined from OCR. The excess pore pressure is equal to μ times the settlement and the excess pore water pressures by Skempton and Bjerrum's three-dimensional method were 42 kPa and 38 kPa at 3m and 6m depth, respectively. Consequently, the Skempton and Bjerrum (1957) method were agreed well with the observed data at 3m and 6m depth. The comparison of excess pore water pressures between the average observed field data, the FEM 2D and 3D simulation variations and Skempton and Bjerrum's three-dimensional method with time were plotted in **Fig. 14** for 3m depth and **Fig. 15** at 6m depth.

5.2 Hexagonal wire mesh reinforced embankment

The hexagonal wire mesh reinforced embankment (**Fig. 16**) was constructed at the northern part of the campus of the Asian Institute of Technology (AIT). The

Fig. 16. Completed hexagonal wire mesh reinforced embankment (Teerawattanasuk, 2004).

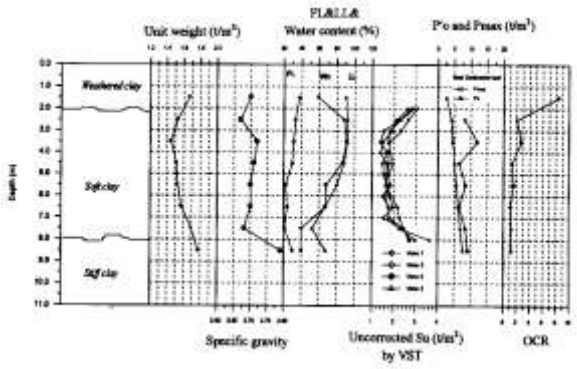

Fig. 17. General soil profile and properties of the subsoil at Asian Institute of Technology (AIT) (Chai 1992; Bergado et al. 1995).

general soil profile and soil properties of the subsoil in the uppermost 3 layers at the AIT campus are presented in Fig. 17. The uppermost 12 m can be divided into 5 layers (**Table 3**). Weathered crust consisting of heavily overconsolidated reddish brown clay forms the uppermost 2m constitutes the first and second layers. This layer is underlain by a soft, grayish clay from 2.0 to 6.0 m depth as the third layer. The medium stiff clay with silt seams and fine sand lenses was found at 6.0 to 8.0 m depth as layer 4. Below this layer from 8.0 to 12.0 m is the stiff clay layer as layer 5 (Teerawattanasuk, 2004).

The hexagonal wire mesh reinforced embankment was 6.0 m high, 6.0 m long at the top, top width of 6.0 m, and base width of 18.0 m as illustrated in Fig. 18. A fully instrumented test embankment with hexagonal wire mesh as the reinforcement was completed within 60 days period (Voottipruex 2000). After 405 days of construction, the top of the embankment was raised up by 1 m as an addition surcharge load to investigate its behavior. The embankment was divided into two parts along its length. Zinc-coated and PVC-coated hexagonal wire mesh reinforcements were used in each respective portion with the same backfill material (Ayutthaya sand). The gabion facing of the embankment was built with 10 degrees inclination from the vertical alignment. The side slope and back slope were 1:1 as shown in **Fig. 19.** The facing was

made from large rectangular wire mesh baskets wired together and filled with crushed rock (Bergado et al. 2000). The locations of the instruments for monitoring the embankment behavior such as settlement and excess pore water pressure are illustrated in **Fig. 19.**

5.2.1 Numerical simulations

Based on the work of Teerawattanasuk (2004), the numerical simulations of the hexagonal wire mesh reinforced embankment were done using 2D at 3D explicit FD softwares FLAC^{2D} (ITASCA FLAC2D version 3.4, 1998) and FLAC^{3D} (ITASCA FLAC3D version 2.0, 1997). The finite difference technique (2D and 3D numerical modeling) have been applied to simulate the behavior of hexagonal wire mesh reinforced embankment in term of vertical settlements and excess pore-water pressures. The 3D finite difference discretization for the hexagonal wire mesh reinforced embankment is shown in **Fig. 20.** The hexagonal wall facing system was also characterized by the solid elements. However, the linear elastic-perfectly plastic, Mohr-Coulomb model was used to simulate the hexagonal wall facing system based on the study of Bergado et al. (2000). According to the Mohr-Coulomb failure criterion, a constraint of failure was recognizing a "tension cutoff" superimposed on the Mohr-Coulomb failure criterion. Both undrained and consolidation analyses were carried out in the consecutive steps of the numerical analysis. The undrained analysis was performed until the maximum excess pore-water pressure can be achieved. The consolidation analysis was then started continuously to dissipate the excess pore-water pressure within the considered time. The input parameters of backfill for the FLAC^{2D} and FLAC^{3D} finite difference technique are tabulated in **Table 3.** The permeability values of foundation soils ($k = 25\ k_v$) were applied in the numerical analyses. Comparisons between findings of 2D and 3D numerical results and the measured field data (vertical settlements and excess pore-water pressures) are discussed in the following sections.

5.2.2 Settlements

Underneath the center point of the hexagonal wire mesh reinforced embankment, **Figs. 21** and **22** show the comparison of predicted and measured surface settlement (0.45 m depth below the original ground surface, refer to settlement plate S2) as well as two subsurface settlements (3 m depth below the original ground surface, refer to settlement plate SS1), respectively.

Referring to **Figs. 21** and **22,** it can be observed that the predicted values of surface settlements obtained from 3D numerical analyses were closer and slightly overestimated the measured data than the predicted results obtained from 2D numerical analyses. However, the actual settlement patterns for this embankment were

Table 3. Soil models and parameters used in finite difference analyses on full-scale hexagonal wire mesh reinforced embankment test.

Parameters	Symbol	Soil Layer					Wall Face	Backfill
		1	2	3	4	5		
	Depth (m)	0-1	1-2	2-6	6-8	8-12		
Soil Model		MC[1]	MCC [2]				MC[1]	MC[1]
Slope of Elastic Swelling line	κ		0.04	0.11	0.07	0.04		
Slope of Normal Consolation Line	λ		0.18	0.51	0.31	0.18		
Frictional Constant	M		1.1	0.9	0.95	1.1		
Specific Volume at Reference Pressure (1Pa)	v_λ		4.256	8.879	5.996	4.168		
Reference Pressure (1Pa)	p_1		1	1	1	1		
Poisson's Ratio	ν	0.25	0.25	0.3	0.3	0.25		
Maximum Elastic Bulk Modulus (x10^7 Pa)	κ_{max}		12.5	2.88	4.86	9.6		
Preconsolidation Pressure (x10^4 Pa)	p_{co}		14.3	7.55	9.3	10.7		
Elastic Bulk Modulus (x10^6 Pa)	K	2.67					5.88	5
Elastic Shear Modulus (x10^6 Pa)	G	1.6					2.69	2.31
Friction Angle, (degree)	ϕ'	29					45	30
Cohesion, (x10^3 Pa)	c'	29					20	10
Total Unit Weight (kg/m^3)	ρ_τ	1750	1750	1500	1650	1750	1800	1800
Dry Unit Weight (kg/m^3)	ρ_d	1750	1750	803	1050	1226	1800	1800
Porosity	n	0.545	0.545	0.697	0.6	0.524		
Permeability (x10^{-12} m^2/(Pa sec))	$25.0k_v$	17.8	17.8	2.65	2.65	17.8		

MC[1]: Elastic Perfectly Plastic Mohr-Coulomb Model; MCC[2] :Modified Cam-Clay Model.

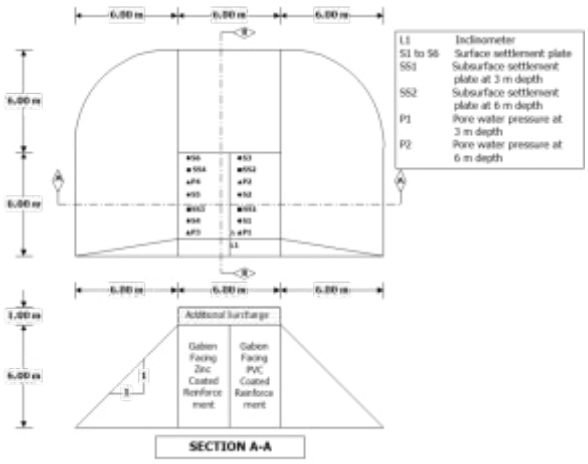

Fig. 18. Section A-A view of hexagonal wire mesh reinforced embankment.

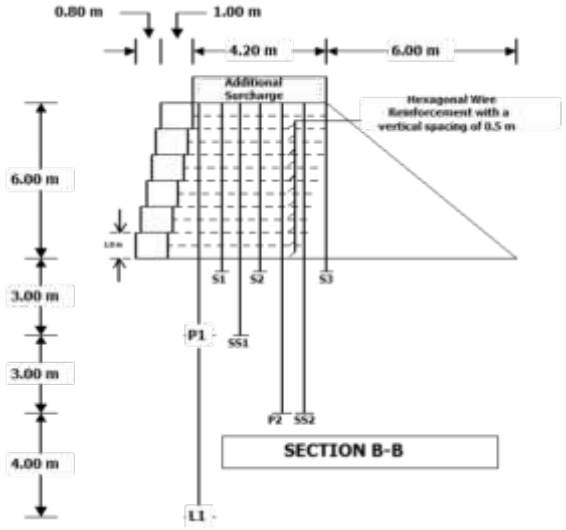

Fig. 19. Section B-B view of hexagonal wire mesh reinforced embankment.

closely related to 3D analyses. Thus, the embankment geometry (2D vs 3D) can be an important factor that influences the predicted results. According to the principle from Skempton-Bjerrum (1957) as shown in **Fig. 3,** the average OCR = 2 (at 0.45 m depth or ground surface) for the whole soft clay layer corresponding to pore pressure parameter of 0.58 in **Fig. 4.** The ratio of 2D to 3D settlement in **Fig 21** is 4.0/7.1 = 0.56 which is near to 0.58. While, the average OCR = 1.8 from 3m to 8m depths corresponding to pore pressure parameter of 0.60. The corresponding ratio of 2D/3D at 3m depth (**Fig. 22**) is 2.9/5.4 = 0.54 which is near to 0.60, as illustrated in **Fig. 23.**

5.2.3 Excess pore-water pressures

Figure 24 shows the comparison of excess pore-water pressure variations with time together with the measured field data of the hexagonal wire mesh

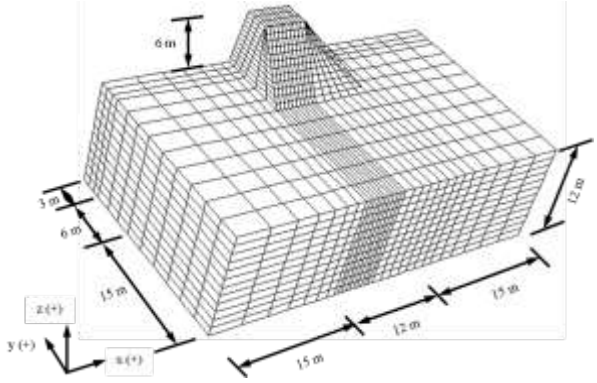

Fig. 20. 3D finite difference grid discretization for hexagonal wire mesh reinforced embankment with FLAC^{3D} (Analysis No. 6).

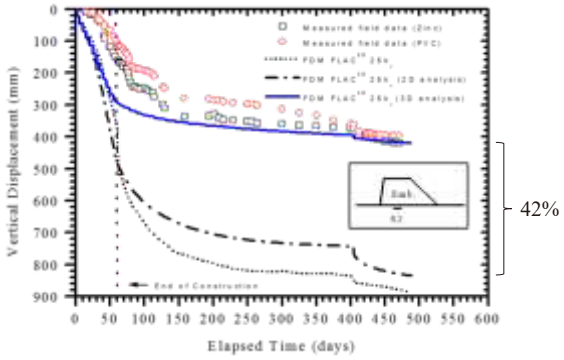

Fig. 21. Comparison of measured and predicted surface settlement of hexagonal wire mesh reinforced embankment under 2D and 3D analyses at settlement plate 0.45m depth.

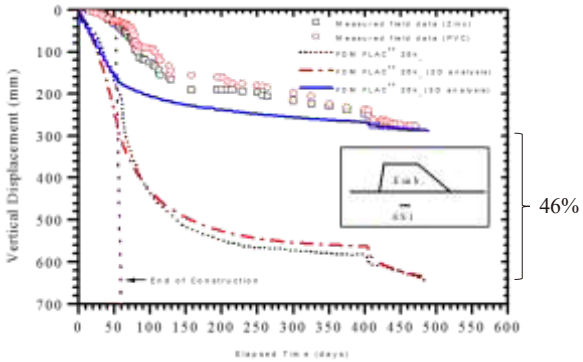

Fig. 22. Comparison of measured and predicted subsurface settlement of hexagonal wire mesh reinforced embankment under 2D and 3D analyses at settlement plate 3m depth.

reinforced embankment for the hydraulic piezometer, P1 (3.0 m depth below the original ground surface).

Referring to **Fig. 24** at the end of construction (at the elapsed time of 60 days), the predicted maximum excess pore-water pressure at the locations of P1 obtained from 2D numerical analyses overestimated the measured field data while the predicted values from 3D analysis yielded satisfactory agreement. Due to the dissipation of pore-water pressures after the end of construction, analysis schemes have higher dissipation rate than the measured

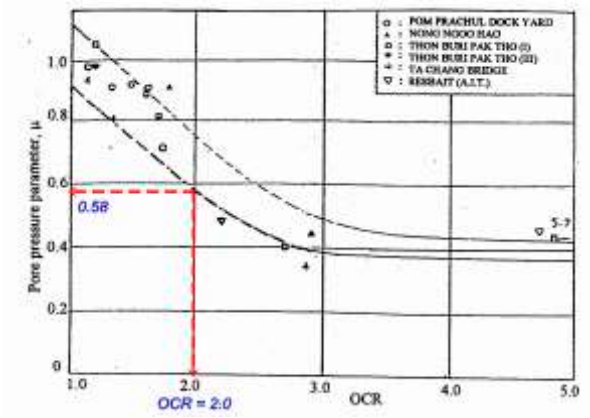

(a) at 0.45m depth

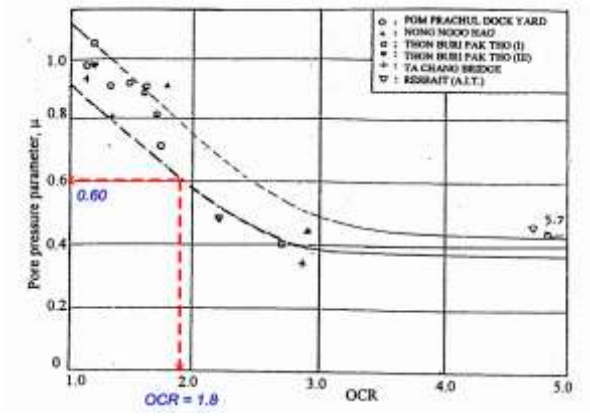

(b) at 3m depth

Fig. 23. The correction factor (μ) with overconsolidation ratio of hexagonal wire mesh reinforced embankment.

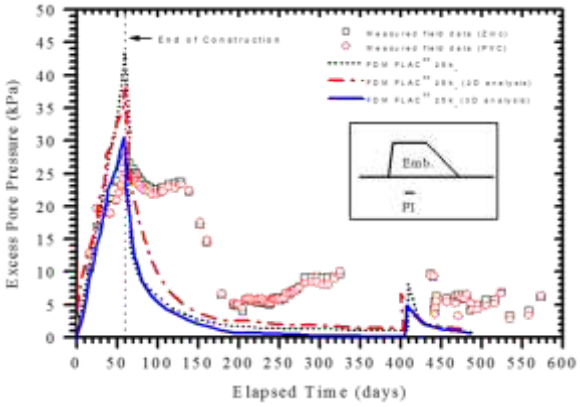

Fig. 24. Comparison of measured and predicted excess pore-water pressure of hexagonal wire mesh reinforced soil embankment under 2D and 3D analyses at 3 m depth.

field data which caused lower predicted values compared to the dissipation of excess pore-water that occurred in the field. Subsequently, at the elapsed time of 405 days, the additional surcharge was added. Then, the excess pore-water pressures increased again and started to continually dissipate with time. Considering the embankment during construction (at the elapsed time 0 to 30 days), the rate of excess pore-water pressure dissipation under plane strain condition is lower than the 3D analysis because the excess pore-water pressure can dissipate only in two directions (in x and z directions) in the former while the excess pore-water pressures can dissipate in all directions (x, y, and z directions) in the latter.

6. Summary

The LLGs reinforced embankment (Chaiyaput et al, 2014) was constructed by using silty sand backfill until 3 m height and covered by 1m thick compacted weathered clay at the top, back and side slope with a total height of 4 m (**Figs. 8** and **9**). It has 4.0 m x 5.0 m dimensions at the top and 16.0 m x 15.0 m at the base (**Fig. 7**). Moreover, the side and back slopes consisted of 1 vertical to 1.5 horizontal and the front slope consisted of 1 vertical to 1 horizontal. The embankment with hexagonal wire mesh reinforcement (**Fig. 16**). was also constructed on the AIT campus (Voottipruex 2000). The embankment was 6.0 m high, with 6.0 m by 6.0 m top dimensions and 12.0 m by 18.0 m base dimensions (**Fig. 18**). The top of the embankment was raised up by 1 m as an additional surcharge load to investigate its behavior. The gabion facing of the embankment was built with 10 degrees inclination from the vertical alignment. The side slope and back slope were 1:1. The settlement magnitude of 6.0 m high hexagonal wire mesh reinforced embankment is higher than the settlement magnitudes of 4.0 m high Kenaf LLGs reinforced embankment. Moreover, the observed and predicted data of surface and subsurface settlements obtained from 3D simulation agreed well compared to the 2D simulation due to the 3D geometric effects and short plan dimensions of the test embankment. The difference of final settlements between 2D and 3D FEM simulations at the surface and subsurface locations were agreed with the Skempton and Bjerrum corrections.

The simulations of excess pore water pressures from 3D simulations agreed well with the observed data at 3.0 m and 6.0 m depths due to the similarities of the 3D boundary conditions in the field.

The OCR values of Kenaf LLGs embankment is 1.55, 1.40 and 1.30 for soft clay layer at the surface 3m and 6m depths, respectively. The OCR values of hexagonal wire mesh embankment is 2.00 and 1.80 for soft clay layer at the 0.45m and 3m depths, respectively. It can be seen that the settlements predictions of the soft clay foundation mostly depended on the overconsolidation ratios of the underlying soft clay layer.

The settlement at 2D and 3D conditions can be calculated by using Skempton and Bjerrum (1957) method. A correction factor (μ) should be applied to the settlement calculated on the basis of odometers test and plane strain conditions. The correction factor (μ)

decreased with increasing overconsolidation ratio (OCR). The amount of loading affects to settlement, pore pressure, and OCR of the soil properties. The Skempton and Bjerrum corrections were confirmed by the results of the 2D and 3D FEM as well as 2D and 3D FD simulations of full scale embankments.

7. Conclusions

The prediction of final settlements of 3D numerical simulation was proposed by applying the 2D numerical simulation with the corrections values from Skempton and Bjerrum theorem. The following conclusions can be made:

1. The 3D numerical simulation captured the overall behavior of the embankments with 3D configuration, especially the behavior of short embankment (length-to-width ratio of 1.0).

2. The Skempton-Bjerrum 2D to 3D correction method agreed with the final settlements in 2D and 3D numerical simulations of full scale embankments and confirmed by field observations.

Consequently, it was confirmed that the Skempton-Bjerrum method provides reasonable results supported by the measured data from full scale embankments and can be used to calculate the final settlement from 2D to 3D configurations.

References

Auvinet and Gonzalez., 2000. Three-dimensional reliability analysis of earth slopes. Computers and Geotechnics, **26**: 247–261.

Bergado, D.T., and Teerawattanasuk, C., 2008. 2D and 3D numerical simulations of reinforced embankments on soft ground. Geotextiles and Geomembranes, **26** (1): 39–55.

Bergado, D. T., Teerawattanasuk C., Youwai S. and Voottipruex P., 2000. FE modeling of hexagonal wire reinforced embankment on soft clay. Canadian Geotechnical Journal, **37**: 1209-1226.

Bergado, D. T., Chai, J. C. and Miura, N., 1995. FE Analysis of grid reinforced embankment system on soft Bangkok clay. Computers and Geotechnics, **17**: 447-471.

Bjerrum, L., 1972. Embankment on soft ground, Proc. ASCE Conf. on Performance of Earth Support Structure, Purdue University, Lafayette, Indiana, 2: 1-54.

Biot, M. A., 1941. General theory of three dimensional consolidation, Journal of Applied Physics, **12**: 155-164.

Britto, A. M. and Gunn, M. J., 1987. Critical State Soil Mechanics via Finite Elements. Ellis Horwood, Chichester, U.K.

Chai, J. C., 1992. Interaction Behavior between grid reinforcement and cohesive frictional soils and performance of reinforced wall/embankment on soft ground. D. Eng Dissertation No. GT-91-1, Asian Institute of Technology, Bangkok, Thailand.

Chaiyaput, S., Bergado, D. T., and Artidteang, S., 2014. Measured and simulated results of a Kenaf Limited Life Geosynthetics (LLGs) reinforced test embankment on soft clay, Geotextile and Geomembranes, **42** (1): 39-47.

D' Appolonia, D. J., Poulos, H. G. and Ladd, C. C., 1971. Initial settlements of structure on clay, Journal of the Soil Mechanics and Foundation Division,: 1359-1376.

Hird, C. C, and Kwok, C. M., 1989. FE studies of interface behavior in reinforced embankments on soft ground, *Computers and Geotechnics,* **8**: 111-131.

ITASCA, FLAC2D Version 3.4, 1998. Fast Lagrangian Analysis of continua in 2 Dimensions. ITASCA Consulting Group Inc.

ITASCA, FLAC3D Version 2.0, 1997. Fast Lagrangian Analysis of continua in 3 Dimensions. ITASCA Consulting Group Inc.

Jostad, H.P., Sivasithamparam, N., Woldeselassie, B.H., Lacasse, S., 2016. 3D FE tool for time dependent settlement predictions, Proc. of the 17th Nordic Geotechnical Meeting Challenges in Nordic Geotechnic, May 25th - May 28th, 2016, Reykjavik, Iceland.

Lai, Y. P., Bergado, D. T., Lorenzo, G. A., and Duangchan, T., 2006. Full-scale reinforced embankment on deep jet mixing improved ground. Ground Improvement, **10** (4): 153-164.

Long, P. V., Bergado, D. T. and Balasubramaniam, A. S., 1996. Stability analysis of reinforced and unreinforced embankments of soft ground. Geosynthetics International, **3** (5): 583–604.

Mesri, G., 1973. Coefficient of secondary compression, Journal of the Soil Mechanic and Foundations Division, ASCE, **99** (SM1): 122-137.

Rowe, R. K. and Ho, S. K., 1997. Continuous panel reinforced soil walls on rigid foundations. Journal of Geotechnical and Geoenvironmental Engineering, ASCE, **123** (10): 912-920.

Skempton, A. W., 1954. The Pore Pressure Coefficients A and B. Geotechnique, **4**: 143-147.

Skempton, A. W. and Bjerrum, L., 1957. A contribution to the settlement analysis of foundations on clay.

Geotechnique, **7** (4): 168-178.

Tanchaisawat T., Bergado D. T., and Voottipruex P., 2009. 2D and 3D simulation of geogrid-reinforced geocomposite material embankment on soft Bangkok clay. Geosynthetics International, **16** (6): 420-432.

Teerawattanasuk, C., 2004. Modeling of hexagonal wire reinforcedment and 2D/3D simulation of full scale embankment. D. Eng Dissertation No. GE-03-03, Asian Institute of Technology, Bangkok, Thailand.

Vermeer, P. A. and Brinkgreve, R. B. J. (Editor), 1995. Finite Element Code for Soil and Rock Analysis, A. A. Balkema, Rotterdam, Netherland.

Voottipruex, P., 2000, Interaction of hexagonal wire reinforcement with silty sand backfill soil and behavior of full scale embankment reinforced with hexagonal wire, D.Eng. dissertation GE-99-1, Asian Institute of Technology, Bangkok, Thailand.

Symbols and abbreviations

ρ_t	total ultimate settlement
ρ_i	immediate settlement resulting from the constant volume distortion of the loaded soil mass
ρ_c	consolidation settlement resulting from the time dependent flow of water from the loaded area under the influence of the load that generate excess pore pressure which in itself dissipated by the flow
ρ_s	secondary settlement or creep which is also time dependent but may occur at essentially constant effective stress
$\rho_{c(oed)}$	consolidation settlement on the basis of oedometer tests;
σ_p	maximum past pressure
σ_v	the increase in vertical stress due to embankment loading
$\Delta\sigma_1, \Delta\sigma_3$	the increase in the principle stresses caused by loading
μ	the pore pressure correlation factor
A, B	the pore pressure coefficients
E	modulus of elasticity
ν	the undrained Poisson's ratio
q	the net load on foundation
B	dimension of contributing the loaded area
I	influence value, depending on the shape of the loaded area and the depth of the clay bed
K_o	major principal effective stresses
dz	the vertical compression of a soil element of thickness
m_v	coefficient of volume compressibility in vertical
C_α	secondary compression index
Δe	change of void ratio
t_2, t_1	time
e_p	void ratio at the end of primary consolidation
k_x	permeability in x-direction
k_y	permeability in y-direction
p,$p_{steady\ state}$	pore water pressure
n	porosity
ε	strain tensor
k_w	bulk modulus of water